Measurement and Analysis of the Fermi Resonance between ν_5 and $2\nu_9$ of Nitric Acid

A. G. MAKI[1]

Molecular Spectroscopy Division, National Institute of Standards and Technology, Gaithersburg, Maryland 20899

AND

J. S. WELLS

Time and Frequency Division, National Institute of Standards and Technology, Boulder, Colorado 80303

New tunable diode laser measurements have been made on the ν_5 and $2\nu_9$ infrared absorption bands of HNO$_3$ between 853 and 919 cm^{-1}. These two bands are observed to be about 17 cm^{-1} apart and are coupled by Fermi resonance which causes a considerable displacement of all the energy levels and transition frequencies. An effective resonance interaction of the type $\langle \nu_5, J, k + 2 | 2\nu_9, J, k \rangle$ is particularly important for understanding the appearance of the spectrum. The Fermi resonance has been taken into account in a global fit of both bands that has allowed us to assign all of the strongest transitions. The Fermi interaction constant found is $W_f = 8.13 \pm 0.14$ cm^{-1} and the unperturbed band separation is 6.0 ± 0.4 cm^{-1}. Other higher-order interactions were also considered in the analysis, including a $\Delta K = \pm 2$ Coriolis interaction. Over 1400 diode laser transitions were fitted with a rms deviation of 0.00099 cm^{-1}. Transition wavenumbers, assignments, and lower state energies are made available for the strong transitions of HNO$_3$ between 853 and 920 cm^{-1}. © 1992 Academic Press, Inc.

I. INTRODUCTION

Murcray *et al.* (*1*) have shown that between 850 and 920 cm^{-1} the infrared spectrum of the Earth's atmosphere at certain altitudes is dominated by the absorption of the ν_5 and $2\nu_9$ bands of nitric acid (HNO$_3$). Because of the importance of HNO$_3$ in the chemistry of the upper atmosphere, a number of workers have used that spectral region to measure the spatial and temporal distribution of HNO$_3$ in the atmosphere (*2–7*). In spite of the interest in the ν_5 and $2\nu_9$ band system, there has been no satisfactory analysis of the spectrum that would allow one to assign quantum numbers to the energy levels involved in the stronger transitions.

In an early report on infrared measurements that showed some rotational structure, Chevillard and Giraudet (*8*) gave a crude analysis in terms of assigning *P*-, *Q*-, and *R*-branch features to either ν_5 or $2\nu_9$. At about the same time Brockman *et al.* (*9*) published the high-resolution spectrum between 891 and 899 cm^{-1} measured with a tunable diode laser. They offered no assignments for the observed features. In two subsequent papers the measurements of Brockman *et al.* (*9*) were given assignments by Dana (*10, 11*). Unfortunately, Dana's assignments for $2\nu_9$ were flawed by the assumption that *c*-type transitions were possible. Dana also thought that he had found some *b*-type transitions for ν_5, whereas we believe that those transitions were misassigned.

---

[1] Present address: 15012 24 Ave. S.E., Mill Creek, Washington 98012.

The diode laser spectrum of $2\nu_9$ has also been measured by Giesen et al. (12) who found that some of the lines were easily assigned and fit, while many others could not be assigned because of the displacement caused by the Fermi resonance with ν_5. They found that most of the $2\nu_9$ lines are split into close doublets by the inversion of the hydrogen atom position. We have observed the same doublet splittings for most of the $2\nu_9$ transitions.

In the first phase of the present work new diode laser measurements were given for ν_5 and the role of Fermi resonance in causing a perturbation in the $K_a > 2$ levels near $J = 24$ was explained for the first time (13). That paper not only assigned the new measurements, including the Q-branch region of ν_5, but also assigned those lines due to ν_5 in the spectrum given by Brockman et al. (9).

In this paper we report new diode laser measurements on ν_5 and $2\nu_9$ and the assignment of some of the Q-branch features observed for $2\nu_9$. We also report the results of a complete analysis of both bands including the global effects of both a Fermi-resonance matrix element and a $\Delta K = 2$ Coriolis-resonance matrix element. The present work confirms and extends our earlier assignments for ν_5 and presents a set of effective deperturbed (or unperturbed) rovibrational constants for the $v_5 = 1$ and $v_9 = 2$ states based on a fit of about 1400 tunable diode laser measurements. The present analysis includes 72 microwave measurements given us by Frank C. De Lucia and is consistent with FTS measurements made by Aaron Goldman et al. between 850 and 920 cm^{-1}.

II. EXPERIMENTAL DETAILS

The tunable diode laser measurements were made in both the NIST-Gaithersburg and NIST-Boulder laboratories and were described in our earlier paper (13). The calibration was provided by OCS absorption lines in the region below 891 cm^{-1} and by N_2O absorption lines above 891 cm^{-1}. The OCS calibration frequencies were based on heterodyne frequency measurements made by Wells and co-workers (14, 15). The N_2O calibration data were calculated from the constants given by Maki et al. (16), which were also based on frequency measurements.

Many of the features used in the present analysis were weaker transitions and were not single lines; consequently, the standard deviation was not expected to be as good as that found in the earlier work on ν_5 (13). We believe that the rms deviation of 0.00099 cm^{-1} for the diode measurements correctly reflects the measurement uncertainty due to such problems as poor signal-to-noise ratio for weak transitions, incompletely resolved overlapping lines, and calibration difficulties.

III. ASSIGNMENTS

Both ν_5 and $2\nu_9$ have A' symmetry, which means that they are in-plane vibrations that may give rise to hybrid A- and B-type bands. We find that both bands are primarily A-type bands because the strongest transitions that are uniquely b-type (13), transitions of the type $(J, K_a = J, K_c = 0, 1 \leftarrow J \pm 1, K_a = J \pm 1, K_c = 1, 0)$, are either missing or very weak.

To understand the assignments and the $\Delta K = 2$ perturbation effects one should study our earlier paper (13). Although earlier assignments were taken into account, the entire assignment process for all the transitions was begun anew for the present work. Initially the Q-branch transitions were left out of the fit and a good estimate of the A rotational constant was assumed. The beginning of the Q-branch structure was

sufficiently abrupt to indicate the band center position for each band, thus allowing one to assign the J numbering for the P- and R-branch clusters. The K numbering within the P- and R-branch clusters was also fairly obvious once the pattern within one cluster had been recognized. For ν_5 that pattern has been described earlier (13). Figure 1 shows the form and assignments for a typical high-J P-branch cluster. For $2\nu_9$ the pattern is similar except that the $K_a = 0$, 1 transitions are at the high-frequency end of the cluster, just the opposite from what is found for ν_5.

Most of the $2\nu_9$ transitions are split or noticeably broadened by the splitting due to the double minimum potential for the two equivalent hydrogen atom positions in the plane of the molecule. This splitting, or broadening, aided in identifying the $2\nu_9$ transitions. As indicated by Giesen et al. (12) the splitting seems to be greatest for $K_c = J$ and smallest for $K_c = 0$. The Q-branch transitions seem to show no splitting as would be expected because they involve the smallest values of K_c.

Because of the prior analysis of the displacement of the lines of ν_5 in the region of the $\Delta K = 2$ perturbation, the complementary displacement pattern of the $2\nu_9$ lines was easy to recognize. In some cases combination-differences were used to verify the assignments, especially for the more highly perturbed transitions for which the assignments were not always obvious. One problem with very dense spectra is that one can usually find a line within 0.01 cm^{-1} of a predicted position and one can often predict two possible transitions for a given observed feature. This gives a certain degree of ambiguity to all but the strongest transitions. In addition, hot band transitions due to the low-frequency torsional vibration, as well as two other vibrational states below 700 cm^{-1}, provide a background of weak transitions throughout the spectrum. Because of these hot band transitions, we have made no effort to assign all of the transitions observed.

Transitions involving levels up to $J = 56$, $K_a = 0$, and $K_c = 56$ were assigned and fit for ν_5 and transitions involving levels up to $J = 59$, $K_a = 0$, and $K_c = 59$ were assigned and fit for $2\nu_9$. The maximum value observed for K_a was 36 for ν_5 and 37 for $2\nu_9$.
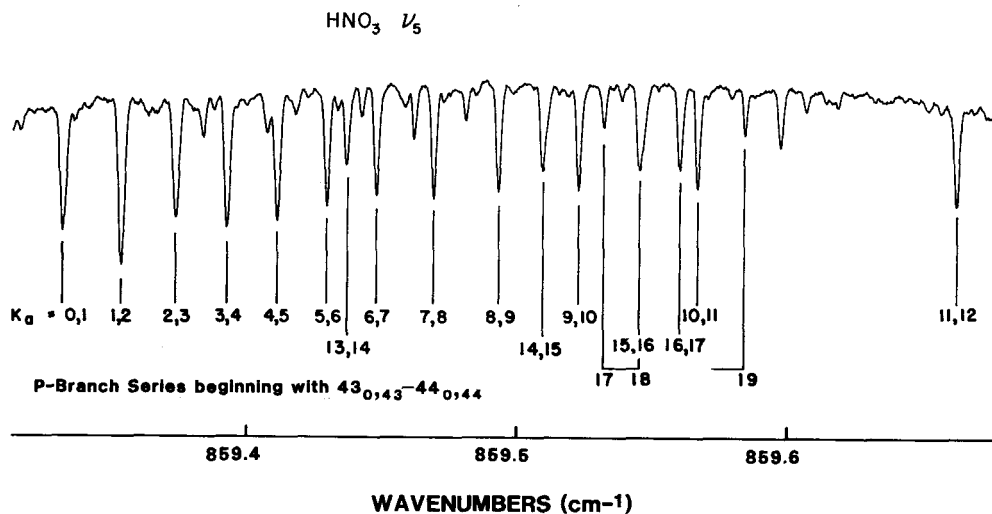

FIG. 1. Spectrum of the low-K_a transitions for the P-branch cluster of ν_5 beginning with the $43_{0,43}$–$44_{0,44}$ and $43_{1,43}$–$44_{1,44}$ transitions at 859.3363 cm^{-1}. For this cluster, the perturbed crossing can be seen to be between $K_a = 11$, 12 and $K_a = 13$, 14 and occurs at $J = 32$.

IV. HOW THE SPECTRUM WAS FIT

Both the $v_5 = 1$ and the $v_9 = 2$ states of HNO_3 are of the same symmetry class, A', so a purely vibrational term in the potential function may be expected to couple the two states. Such terms, usually called Fermi-resonance terms, are expected to have magnitudes on the order of 5 to 30 cm^{-1}. Since the observed (perturbed) separation of the two bands is about 17 cm^{-1}, the Fermi-resonance parameter must be equal to, or smaller than, half that value (i.e., ≤ 8.5 cm^{-1}).

In the absence of rotational crossing effects, a Fermi resonance can usually be taken into account by using effective rotational and centrifugal distortion constants without even using a Fermi-resonance coupling parameter. That means that if the two states do not cross somewhere within their rotational manifold the Fermi-resonance parameter is usually unobtainable unless it can be determined from some kind of evaluation of the vibrational potential function. In the present case there is a crossing between the $K_a + 2$ levels of v_5 and the K_a levels of $2v_9$. The crossing occurs at $J = 22$, for $K_a = 2, 3$ of v_5, but at higher J values for larger K_a, occurring at $J = 31$ for $K_a = 12, 13$ of v_5. Although the Fermi resonance does not directly couple those two nearly degenerate states, the energy matrix for an asymmetric rotor does include $\Delta K = \pm 2$ matrix elements. Consequently, the Fermi resonance does, indirectly, couple the $K_a \pm 2$ levels of v_5 to the K_a levels of $2v_9$. One also could consider this to be a coupling between K_c and $K_c \pm 2$. This coupling could explain the observed perturbations shown in Fig. 1 of Ref. (13) although detailed calculations, such as the present fit, are needed to find if it is adequate.

In the classical case of Fermi resonance, namely CO_2, the resonance has a small dependence on $J(J + 1)$ (17) so we know that constants dependent on J and K should be included. To take into account these higher-order rotational dependencies of the Fermi resonance we have fit the data with the Fermi-resonance matrix elements

$$F_K = \langle v_5, J, k | 2v_9, J, k \rangle = W_f + W_J J(J + 1) + W_K k^2. \tag{1}$$

Here we have used the untransformed, signed, k quantum number.

An alternative explanation for the observed avoided crossings might invoke a Coriolis coupling term. One can show that a purely Coriolis term may directly couple k of $2v_9$ with $k \pm 2$ of v_5. That term would have a matrix element of the form

$$C_{k,k\pm 2} = \langle v_5, J, k \pm 2 | 2v_9, J, k \rangle$$

$$= W_c \{ [J(J + 1) - k(k \pm 1)][J(J + 1) - (k \pm 1)(k \pm 2)] \}^{1/2}. \tag{2}$$

Here the Coriolis term $C_{k,k\pm 2}$ should not be confused with the rotational constant C.

To fit the spectrum we have constructed a nonlinear least-squares fitting program that fits two asymmetric rotors coupled by both Fermi-, $\Delta K = 0$, and Coriolis-, $\Delta K = \pm 2$, resonance matrix elements. This program ignores the torsional splitting of the $v_9 = 2$ state and preserves the separation into E^+, E^-, O^+, and O^- blocks. Figures 2 and 3 indicate the form of three of the energy matrices used by the fitting program. The E^- block is the same as the E^+ block except that the $K = 0$ rows and columns are left out. In Figs. 2 and 3 the upper left quadrant is the same as the normal block for v_5 and the lower right quadrant is the same as the normal block for $2v_9$. Our approach is somewhat different from that of Perrin et al. (18) because we wanted to preserve the full Wang separation and because we found that this approach gives a good fit to the data.

K	0	2	4	0	2	4
0				F_0	$2^{1/2}C_{02}$	0
2		ν_5		$2^{1/2}C_{02}$	F_2	C_{24}
4				0	C_{24}	F_4
0	F_0	$2^{1/2}C_{02}$	0			
2	$2^{1/2}C_{02}$	F_2	C_{24}		$2\nu_9$	
4	0	C_{24}	F_4			

FIG. 2. The E^+ matrix for $J = 4$ with Fermi-resonance coupling terms, F_K, and Coriolis coupling terms, $C_{K,K\pm2}$. The upper left and lower right blocks are the usual, unperturbed E^+ blocks for $J = 4$ of ν_5 and $2\nu_9$, respectively.

As indicated by Pickett (*19*) one of the problems that must be confronted in such a perturbation analysis is how to associate each eigenvalue with the correct quantum numbers and especially with the correct transition. In this particular case the eigenvectors were used to associate each eigenvalue with either ν_5 or $2\nu_9$ according to which has the greater contribution. Then the K_a and K_c quantum numbers were assigned by assuming that the ordering of the energy levels is not changed by the perturbation, for a given value of J within a given vibrational state. This technique worked most of the time as long as the initial estimates of the constants were not very different from the "true" constants.

The perturbed system being fit is very nonlinear because a line that is pushed down by the perturbation can often be switched to being pushed up when a small change is made in the rotational constants. Each K_a subband of $2\nu_9$ crosses the perturbing K_a + 2 subband of ν_5 at a different value of J and the crossing points are sensitive to all the constants for each band. In addition, all levels are shifted by more than 5 cm^{-1} by the resonance. If the initial constants do not correctly predict the crossing points, the fit will not converge. Furthermore, the constants are all highly correlated. In the past we have been able to treat nonlinear systems by starting with the most important

K	1	3	1	3
1			$F_1 \pm C_{11}$	C_{13}
3		ν_5	C_{13}	F_3
1	$F_1 \pm C_{11}$	C_{13}		
3	C_{13}	F_3		$2\nu_9$

FIG. 3. The $O^\pm$ matrix for $J = 3$ (or 4) with Fermi-resonance coupling terms, F_K, and Coriolis coupling terms, $C_{K,K\pm2}$. C_{11} is really $C_{1,-1}$ given by Eq. (2).

constants and fitting the lowest rotational states first and then gradually working to higher-order constants and higher rotational states. In the present case, the Fermi-resonance constant can not be determined unless the energy levels at the crossing point, above the crossing point, and below the crossing point are all included in the fit. The fit must also include perturbed transitions for both ν_5 and $2\nu_9$ before the Fermi-resonance parameter is reliably determined.

Fortunately, the $K_a = 0, 1$ $K_c = J$ and the $K_a = 1, 2$ $K_c = J - 1$ levels of ν_5 are not affected by the $\Delta K = 2$ perturbation even though they are affected by the Fermi resonance. Those transitions were used to get started on the initial constants for ν_5. Rather than describe the long process of determining the constants, suffice it to say that this process was carried out in two somewhat different ways in order to guard against the possibility of arriving at a set of constants that defined a least-squares minimum that did not represent the lowest minimum or true solution to this problem. With so many variables that are highly correlated, this is a real danger. Crucial to this analysis was the inclusion of Q-branch transitions for both ν_5 and $2\nu_9$. One subsidiary minimum that was found gave a Fermi-resonance parameter of 6.5 cm^{-1}, but it was unable to predict the Q-branch structure to better than ±0.2 cm^{-1} although it was able to fit the strongest lines of the P and R branches.

Our previous experience with fitting bands of HNO$_3$ and DNO$_3$ (20–22) had indicated that the sextic constants, such as Φ_K or φ_{JK}, were not needed to fit the infrared data. Consequently, the sextic constants were set equal to the ground state constants. Later, the Φ_J term was added to the fit, but it was not determinable even though microwave transitions up to $J = 47$ for ν_5 were included in the fit. The inclusion of more microwave transitions for higher rotational quantum numbers may force later workers to include higher-order constants as well as to modify some of the other simplifying assumptions we have made.

V. INTENSITY BORROWING

The Fermi resonance mixes the wavefunctions of the ν_5 and $2\nu_9$ bands. This mixing will affect the intensities of the two bands. The intensity of each band depends on the square of the transition moment which in turn depends on the dipole matrix element. Since the dipole matrix element involves the wavefunctions of the upper and lower states of a transition, it will be affected when the effective wavefunction of the upper state is a mixture of the wavefunctions for ν_5 and $2\nu_9$.

For the present perturbed system the mixing of the wavefunctions for $J = 0$ is given by

$$\psi_1 = 0.82\psi_1^0 - 0.57\psi_2^0$$

and

$$\psi_2 = 0.57\psi_1^0 + 0.82\psi_2^0$$

where the subscript 1 stands for $2\nu_9$ and 2 stands for ν_5 and the superscript 0 stands for the unperturbed wavefunction.

Since we do not know the unperturbed intensity of either band, it is not possible to predict the intensity that results from the mixing, but we can consider the two extreme cases where the intensity is dominated by either ν_5 or $2\nu_9$. The most likely situation would be for the unperturbed $2\nu_9$ to have nearly zero intensity. Then the intensity ratio $2\nu_9{:}\nu_5$ would be close to $(0.57)^2{:}(0.82)^2$ or about 1:2. If, instead, ν_5 (unperturbed) were assumed to have zero intensity, then the ratio would be reversed,

2:1. For all intermediate cases the intensity mixing would depend on the relative signs of the unperturbed dipole matrix elements as well as on the sign of the mixing coefficients.

VI. RESULTS

Tables I and II give two sets of deperturbed (or unperturbed) rovibrational constants found for ν_5 and $2\nu_9$. These constants were based on least-squares fits in which the ground-state constants were fixed at the values determined earlier from many microwave measurements (20). The fits included the present diode laser measurements and those reported earlier (13), the diode laser measurements published by Giesen et al.

TABLE I

The Deperturbed Rovibrational Constants (in cm⁻¹) for ν_5 and $2\nu_9$ of HNO₃ as Determined for the A Reduction of the I^r Representation: Results of Fit 1

	Ground State[a]	ν_5	$v_5=1$	$2\nu_9$	$v_9=2$
A	0.433 999 899(44)[b]		0.433 468 15(2163)		0.433 844 88(2158)
$A'-A''$			-0.000 531 75(2163)		-0.000 155 02(2158)
B	0.403 609 999(29)		0.403 761 17(1110)		0.397 966 35(1146)
$B'-B''$			0.000 151 17(1110)		-0.005 643 65(1146)
C	0.208 832 419(37)		0.207 981 19(2226)		0.208 449 72(2229)
$C'-C''$			-0.000 851 23(2226)		-0.000 382 70(2229)
$\Delta_J \times 10^7$	2.970 970(170)		3.455 85(3344)		3.586 25(3344)
$(\Delta_J'-\Delta_J'') \times 10^7$			0.484 88(3344)		0.615 28(3344)
$\Delta_{JK} \times 10^7$	-1.516 232(523)		-5.542 2(2488)		-5.482 6(2180)
$(\Delta_{JK}'-\Delta_{JK}'') \times 10^7$			-4.026 0(2488)		-3.966 4(2180)
$\Delta_K \times 10^7$	2.465 743(722)		6.414 9(2663)		5.452 9(2361)
$(\Delta_K'-\Delta_K'') \times 10^7$			3.949 1(2663)		2.987 1(2361)
$\delta_J \times 10^7$	1.262 656 4(270)		1.507 79(1986)		1.567 55(2026)
$(\delta_J'-\delta_J'') \times 10^7$			0.245 14(1986)		0.304 90(2026)
$\delta_K \times 10^7$	2.493 989(152)		1.797 6(1049)		1.345 7(1026)
$(\delta_K'-\delta_K'') \times 10^7$			-0.696 4(1049)		-1.148 3(1026)
$\Phi_J \times 10^{12}$	-0.016 985(294)		[-0.016 985][c]		[-0.016 985][c]
$\Phi_{JK} \times 10^{12}$	0.942 0(158)		[0.942 0]		[0.942 0]
$\Phi_{KJ} \times 10^{12}$	-3.689 2(700)		[-3.689 2]		[-3.689 2]
$\Phi_K \times 10^{12}$	4.178 6(908)		[4.178 6]		[4.178 6]
$\varphi_K \times 10^{12}$	1.792 5(128)		[1.792 5]		[1.792 5]
$L_{JKKK} \times 10^{16}$	0.795(288)		[0.795]		[0.795]
$L_K \times 10^{16}$	-1.271(384)		[-1.271]		[-1.271]
ν_0		884.776 79(73740)[d]		890.779 68(73738)[d]	
ν_0(perturbed)		879.108 49(20)		896.447 98(20)	
W_f		8.133 62(27246)			
$W_J \times 10^4$		0.182(1237)			
$W_K \times 10^4$		-1.944(1403)			
$W_c \times 10^4$		0.507(699)			
number of rotational transitions	72[e]				
number of infrared transitions	1496				
rms deviation of infrared transitions	0.00099cm⁻¹				

a) The ground-state constants were taken from Ref. (20).
b) The uncertainty in the last digits (twice the estimated standard error) is given in parentheses.
c) The values given in square brackets were fixed at the ground-state values.
d) The uncertainty given for the band center does not include the absolute calibration uncertainty which is on the order of ±0.0002 cm⁻¹.
e) All rotational transitions were provided by F. De Lucia.

TABLE II

The Deperturbed Rovibrational Constants (in cm^{-1}) for ν_5 and $2\nu_9$ of HNO$_3$ as Determined for the A Reduction of the I^r Representation: Results of Fit 2

	Ground State[a]	ν_5	$v_5=1$	$2\nu_9$	$v_9=2$
A	0.433 999 899(44)[b]		0.433 465 35(1003)		0.433 847 66(1004)
$A'-A''$		-0.000 534 55(1003)		-0.000 152 24(1004)	
B	0.403 609 999(29)		0.403 762 357(5531)		0.397 965 174(5258)
$B'-B''$		0.000 152 358(5531)		-0.005 644 825(5258)	
C	0.208 832 419(37)		0.207 978 397(6654)		0.208 452 529(6660)
$C'-C''$		-0.000 854 022(6654)		-0.000 379 890(6660)	
$\Delta_J\times10^7$	2.970 970(170)		3.457 82(3088)		3.585 45(2988)
$(\Delta_J'-\Delta_J'')\times10^7$		0.486 85(3088)		0.614 48(2988)	
$\Delta_{JK}\times10^7$	-1.516 232(523)		-5.567 5(2466)		-5.466 3(2145)
$(\Delta_{JK}'-\Delta_{JK}'')\times10^7$		-4.051 3(2466)		-3.950 0(2145)	
$\Delta_K\times10^7$	2.465 743(722)		6.449 7(2397)		5.425 9(2096)
$(\Delta_K'-\Delta_K'')\times10^7$		3.984 0(2397)		2.960 2(2096)	
$\delta_J\times10^7$	1.262 656 4(270)		1.509 44(1626)		1.566 48(1601)
$(\delta_J'-\delta_J'')\times10^7$		0.246 78(1626)		0.303 82(1601)	
$\delta_K\times10^7$	2.493 989(152)		1.793 6(1069)		1.346 9(1034)
$(\delta_K'-\delta_K'')\times10^7$		-0.700 4(1069)		-1.147 1(1034)	
$\Phi_J\times10^{12}$	-0.016 985(294)		[-0.016 985][c]		[-0.016 985][c]
$\Phi_{JK}\times10^{12}$	0.942 0(158)		[0.942 0]		[0.942 0]
$\Phi_{KJ}\times10^{12}$	-3.689 2(700)		[-3.689 2]		[-3.689 2]
$\Phi_K\times10^{12}$	4.178 6(908)		[4.178 6]		[4.178 6]
$\varphi_K\times10^{12}$	1.792 5(128)		[1.792 5]		[1.792 5]
$L_{JKKK}\times10^{16}$	0.795(288)		[0.795]		[0.795]
$L_K\times10^{16}$	-1.271(384)		[-1.271]		[-1.271]
ν_0		884.886 20(872)[d]		890.670 27(875)[d]	
ν_0(perturbed)		879.108 49(20)[d]		896.447 97(20)[d]	
W_f		8.173 16(307)			
$W_K\times10^4$		-1.736 5(410)			
$W_c\times10^4$		0.403 4(131)			
number of rotational transitions	72[e]				
number of infrared transitions	1496				
rms deviation of infrared transitions	0.00099cm^{-1}				

a) The ground-state constants were taken from Ref. (20).
b) The uncertainty in the last digits (twice the estimated standard error) is given in parentheses.
c) The values given in square brackets were fixed at the ground-state values.
d) The uncertainty given for the band center does not include the absolute calibration uncertainty which is on the order of ±0.0002 cm^{-1}.
e) All rotational transitions were provided by F. De Lucia.

(12) (with two lines reassigned), and 72 microwave measurements for the $v_5 = 1$ state given to us by F. De Lucia.

The present analysis has caused us to change some of the high-J assignments for the $K_c = 1$, 2 and $K_c = 2$, 3 subbands of the Q branch for ν_5 from those given in our earlier paper (13). Aside from the $K_c = 0$, 1 subbands, we are still not very confident of the Q-branch assignments for either ν_5 or $2\nu_9$. However, that uncertainty only affects the Q-branch region, which is not very critical for many atmospheric measurements.

During the early stages of this work we were disturbed to find that the correlation matrix has a few entries very close to 0.999 (or −0.999) and a number of others that show a high correlation (greater than 0.9, or −0.9). Eventually it was realized that the nature of a strong Fermi resonance is to cause a high degree of correlation among

TABLE III

Sample Listing of Absorption Line Wavenumbers, Assignments, and Lower State Energies for the ν_5 and $2\nu_9$ Bands of HNO$_3$

Wavenumber (cm⁻¹)	J'	K'$_a$	K'$_c$	vib.'[a]		J"	K"$_a$	K"$_c$	vib."	lower state energy (cm⁻¹)
859.3363	43	1	43	1	-	44	1	44	0	422.52
859.3363	43	0	43	1	-	44	0	44	0	422.52
859.3561	32	12	20	1	-	33	12	21	0	376.48
859.3561	32	13	20	1	-	33	13	21	0	376.48
859.3568	42	1	41	1	-	43	1	42	0	421.73
859.3568	42	2	41	1	-	43	2	42	0	421.73
859.3687	26	24	2	1	-	27	24	3	0	313.65
859.3712	26	24	3	1	-	27	24	4	0	313.65
859.3756	41	2	39	1	-	42	2	40	0	420.09
859.3756	41	3	39	1	-	42	3	40	0	420.09
859.3933	40	4	37	1	-	41	4	38	0	417.62
859.3933	40	3	37	1	-	41	3	38	0	417.62
859.3984	25	20	6	1	-	26	20	7	0	282.01
859.4072	18	10	9	1	-	19	12	8	0	145.26
859.4079	18	9	9	1	-	19	11	8	0	145.25
859.4107	39	4	35	1	-	40	4	36	0	414.30
859.4107	39	5	35	1	-	40	5	36	0	414.30
859.4165	19	16	4	1	-	20	18	3	0	174.62
859.4177	17	7	11	1	-	18	9	10	0	121.98
859.4177	17	6	11	1	-	18	8	10	0	121.98
859.4285	38	6	33	1	-	39	6	34	0	410.14
859.4285	38	5	33	1	-	39	5	34	0	410.14
859.4309	24	18	6	1	-	25	18	7	0	260.09
859.4318	19	13	7	1	-	20	15	6	0	167.51
859.4353	30	13	17	1	-	31	13	18	0	346.59
859.4353	30	14	17	1	-	31	14	18	0	346.59
859.4473	37	6	31	1	-	38	6	32	0	405.14
859.4473	37	7	31	1	-	38	7	32	0	405.14
859.4682	36	8	29	1	-	37	8	30	0	399.30
859.4682	36	7	29	1	-	37	7	30	0	399.30
859.4924	35	8	27	1	-	36	8	28	0	392.62
859.4924	35	9	27	1	-	36	9	28	0	392.62
859.5073	29	15	15	1	-	30	15	16	0	334.85
859.5073	29	14	15	1	-	30	14	16	0	334.85
859.5103	25	21	5	1	-	26	21	6	0	284.75
859.5181	19	16	3	1	-	20	18	2	0	174.62
859.5228	34	10	25	1	-	35	10	26	0	385.10
859.5228	34	9	25	1	-	35	9	26	0	385.10
859.5233	26	17	9	1	-	27	17	10	0	294.41
859.5399	26	18	9	1	-	27	18	10	0	294.41
859.5426	28	16	13	1	-	29	16	14	0	322.25
859.5426	28	15	13	1	-	29	15	14	0	322.25
859.5560	27	16	11	1	-	28	16	12	0	308.78
859.5562	27	17	11	1	-	28	17	12	0	308.78
859.5674	33	10	23	1	-	34	10	24	0	376.74
859.5674	33	11	23	1	-	34	11	24	0	376.74
859.5844	25	19	7	1	-	26	19	8	0	279.08
859.5882	20	14	6	1	-	21	16	5	0	186.24
859.6056	19	12	7	1	-	20	14	6	0	167.32
859.6308	26	25	1	1	-	27	25	2	0	317.35
859.6309	26	25	2	1	-	27	25	3	0	317.35
859.6633	32	12	21	1	-	33	12	22	0	367.53
859.6633	32	11	21	1	-	33	11	22	0	367.53

[a] Vibration number 2 is $2\nu_9$, number 1 is ν_5, and 0 is the ground state.

many constants for ν_5 and their counterparts for $2\nu_9$. That is a consequence of the resonance mixing the two constants such that if one gets smaller, the other must get larger by about the same amount. This is particularly true of the three constants, $\nu_0(\nu_5)$, $\nu_0(2\nu_9)$, and W_f. Of course the sum of the two band centers does not depend on W_f, but the difference does. It is the high correlation that makes the value of the rotational constant C for $2\nu_9$ appear to be as well determined as the value of C for ν_5, even though accurate microwave measurements were available only for ν_5.

The results of two different fits are given in Tables I and II in order to show how the constants and their uncertainties can change as the model used in the fit is changed. In both tables the constants are given with many more figures than the uncertainty

seems to warrant. The high correlation of some of the constants requires the use of all the figures given in Table II in order to correctly calculate the transitions.

In the fit of Table I, labeled Fit 1, both the W_J and the W_c constants were included in the fit. In that fit there is a high correlation between W_J and W_c and neither constant is determined with any degree of confidence. In addition, the main Fermi-resonance constant, W_f, has a rather large uncertainty, as do the band centers. Because of the high correlation, it is recommended that the constants of Table I not be used. In the fit of Table II, Fit 2, the least significant constant, W_J, was left out of the model. In that fit the constant W_c appears to be determined with much greater accuracy and the uncertainties in the band centers and the Fermi-resonance constant, W_f, were improved by factors of 100 or more. The rms deviation was the same for both fits.

We have also made a fit with the W_c term left out but with W_J included. That fit gave the same rms deviation as the other fits. It gave $W_J = -0.703(\pm0.008) \times 10^{-4}$ cm^{-1} and $W_f = 8.3126 \pm 0.0009$ cm^{-1}. Except for the band centers, the other constants are within one standard deviation of the values given in Fit 2.

Because of the interest in HNO_3 transitions between 853 and 920 cm^{-1}, we have prepared a table of transition frequencies, assignments, and lower state energy levels for all the strong transitions in that frequency range. This table is based on the constants from Fit 2. The inversion splitting of the $2\nu_9$ lines is not given in the table. Due to the uncertainties in the Q-branch transitions, we have omitted all Q-branch transitions, so there are gaps in the list of transitions near the two band centers. This table contains more entries than we can publish ($\sim 10\ 000$ transitions), so it is available[2] from the authors in the form of a $5\frac{1}{4}$-in. double-sided, high-density floppy disc produced with DOS 5.0. Table III shows the segment of that table that covers the region of Fig. 1. In addition, the measurements used in the present analysis are included on that floppy disc for anyone interested in using our data.

REFERENCES

1. D. G. MURCRAY, T. G. KYLE, F. H. MURCRAY, AND W. J. WILLIAMS, *J. Opt. Soc. Am.* **59**, 1131–1134 (1969).
2. P. E. RHINE, L. D. TUBBS, AND D. WILLIAMS, *Appl. Opt.* **8**, 1500–1501 (1969).
3. W. J. WILLIAMS, J. N. BROOKS, D. G. MURCRAY, F. H. MURCRAY, P. M. FRIED, AND J. A. WEINMAN. *J. Atmos. Sci.* **29**, 1375–1379 (1972).
4. D. G. MURCRAY, D. B. BARKER, J. N. BROOKS, A. GOLDMAN, AND W. J. WILLIAMS, *Geophys. Res. Lett.* **2**, 223–225 (1975).
5. C. M. BRADFORD, F. H. MURCRAY, J. W. VAN ALLEN, J. N. BROOKS, D. G. MURCRAY, AND A. GOLDMAN, *Geophys. Res. Lett.* **3**, 387–390 (1976).
6. O. LADO-BORDOWSKY AND G. AMAT, *Appl. Opt.* **18**, 3400–3403 (1979).
7. O. LADO-BORDOWSKY, *J. Opt. (Paris)* **11**, 179–193 (1980).
8. J.-P. CHEVILLARD AND R. GIRAUDET, *J. Phys.* **39**, 517–520 (1978).
9. P. BROCKMAN, C. H. BAIR, AND F. ALLARIO, *Appl. Opt.* **17**, 91–100 (1978).
10. V. DANA, *Spectrochim. Acta Part A* **34**, 1027–1031 (1978).

[2] One is on deposit in the Editorial Office of this journal.

11. V. DANA, *Spectrochim. Acta Part A* **37**, 421–423 (1981).

12. T. GIESEN, M. HARTER, R. SCHIEDER, G. WINNEWISSER, AND K. M. T. YAMADA, *Z. Naturforsch. A* **43**, 402–406 (1988).

13. A. G. MAKI AND J. S. WELLS, *J. Mol. Spectrosc.* **108**, 17–30 (1984).

14. J. S. WELLS, F. R. PETERSEN, AND A. G. MAKI, *J. Mol. Spectrosc.* **98**, 404–412 (1983).

15. J. S. WELLS, M. D. VANEK, AND A. G. MAKI, *J. Mol. Spectrosc.* **135**, 84–88 (1989).

16. A. G. MAKI, J. S. WELLS, AND M. D. VANEK, *J. Mol. Spectrosc.* **138**, 84–88 (1989).

17. A. CHEDIN, *J. Mol. Spectrosc.* **76**, 430–491 (1979).

18. A. PERRIN, O. LADO-BORDOWSKY, AND A. VALENTIN, *Mol. Phys.* **67**, 249–270 (1989).

19. H. M. PICKETT, *J. Mol. Spectrosc.* **148**, 371–377 (1991).

20. A. GOLDMAN, J. B. BURKHOLDER, C. J. HOWARD, R. ESCRIBANO, AND A. G. MAKI, *J. Mol. Spectrosc.* **131**, 195–200 (1988).

21. A. MAKI, *J. Mol. Spectrosc.* **136**, 105–108 (1989).

22. T. L. TAN, E. C. LOOI, K. T. LUA, A. G. MAKI, J. W. C. JOHNS, AND M. NOËL, *J. Mol. Spectrosc.* **149**, 425–434 (1991).